University of the
Highlands and Islands
Oilthigh na Gàidhealtachd
agus nan Eilean

UHI Research Database pdf download summary

Faster growth of the major prokaryotic versus eukaryotic CO2 fixers in the oligotrophic ocean

Zubkov, Mikhail V.

Published in:
Nature Communications

Publication date:
2014

Publisher rights:
©2014 The Authors

The re-use license for this item is:
CC BY

The Document Version you have downloaded here is:
Early version, also known as pre-print

The final published version is available direct from the publisher website at:
10.1038/ncomms4776

Link to author version on UHI Research Database

Citation for published version (APA):
Zubkov, M. V. (2014). Faster growth of the major prokaryotic versus eukaryotic CO2 fixers in the oligotrophic ocean. *Nature Communications*, *5*, 1-6. [3776 (2014)]. https://doi.org/10.1038/ncomms4776

General rights
Copyright and moral rights for the publications made accessible in the UHI Research Database are retained by the authors and/or other copyright owners and it is a condition of accessing publications that users recognise and abide by the legal requirements associated with these rights:

1) Users may download and print one copy of any publication from the UHI Research Database for the purpose of private study or research.
2) You may not further distribute the material or use it for any profit-making activity or commercial gain
3) You may freely distribute the URL identifying the publication in the UHI Research Database

Take down policy
If you believe that this document breaches copyright please contact us at RO@uhi.ac.uk providing details; we will remove access to the work immediately and investigate your claim.

Download date: 08. Dec. 2022

1 **Faster growth of the major prokaryotic versus eukaryotic CO_2-fixers in the oligotrophic**

2 **ocean**

3

4 Mikhail V. Zubkov

5

6 National Oceanography Centre, European Way, Southampton, SO14 3ZH, UK

7 E-mail: mvz@noc.ac.uk

8

1 **Abstract**

2 Because maintenance of non-scalable cellular components – membranes and chromosomes –
3 requires an increasing fraction of energy as cell size decreases, miniaturisation comes at a
4 considerable energetic cost for a phytoplanktonic cell. Consequently, if eukaryotes can use
5 their superior energetic resources to acquire nutrients with more or even similar efficiency
6 compared to prokaryotes, larger unicellular eukaryotes should be able to achieve higher
7 growth rates than smaller cyanobacteria. Here, to test this hypothesis, we directly compare
8 the intrinsic growth rates of phototrophic prokaryotes and eukaryotes from the equatorial to
9 temperate South Atlantic using an original flow cytometric $^{14}CO_2$-tracer approach. At the
10 ocean basin scale cyanobacteria double their biomass twice as frequently as the
11 picoeukaryotes indicating that the prokaryotes are faster growing CO_2 fixers, better adapted
12 to phototrophic living in the oligotrophic open ocean – the most extensive biome on Earth.

1 Since the beginning of life on Earth prokaryotes have regulated the main global
2 biogeochemical cycles [1, 2]. However, after the energetically superior eukaryotes [3] had
3 evolved, prokaryotes appeared to lose control over biological CO_2 fixation in all major
4 biomes including the open ocean. Apparently non-scalable cellular components like
5 chromosomes and membranes handicap growth rates of the smaller phytoplankton cells (cell
6 diameter ~ 1 μm) relative to larger cells (cell diameter 4-8 μm) [4, 5]. There is supporting field
7 evidence that phototrophic picoeukaryotes dominate over cyanobacteria in primary
8 production in coastal [6] and certain oceanic regions [7, 8]. On the other hand the above handicap
9 could be counterbalanced by nutrient transport efficiency, which decreases with increase in
10 cell size [9, 10].
11 Direct comparison of *in situ* growth rates of phototrophic prokaryotes and eukaryotes
12 in the oceanic subtropical gyres can show whether prokaryotes or picoeukaryotes are best
13 adapted to oligotrophic conditions. Compared to other oceanic biomes these gyres are
14 seasonally relatively stable and have remained steady for the geological time necessary for
15 biological co-evolution of these organisms to occur. Because biomass growth of both groups
16 primarily depends on photosynthesis, it is justifiable to compare their growth using the CO_2
17 fixation rates. Up to now cellular biomass of oceanic microbes has been calculated from
18 biovolume, determined microscopically [8], or using a change in impedance [6], or by size
19 fractionation [11], and multiplied by a poorly constrained volume-to-carbon conversion factor,
20 derived from culture studies [12], under an assumption that the factor is unaffected by growth
21 conditions.
22 Here, to circumvent the above assumption, a ^{14}C-tracer experimental method, in
23 which cumulative cellular CO_2 fixation was determined at the end of the light period (12 h)
24 and at the end of the following 12 h dark period (24 h), is developed to compare growth and

1 biomass of the smallest oceanic plastidic protists and cyanobacteria. We find that
2 cyanobacteria grow twice as fast as the smallest eukaryotes both in the South Atlantic gyre
3 and in adjacent regions. Despite their protracted co-evolution simple prokaryotic CO_2-fixers
4 outgrow complex eukaryotic CO_2-fixers in the oligotrophic gyre ecosystems highlighting the
5 underrated growth capacity of phototrophic prokaryotes.
6

7 **Results**

8 Prokaryotic and eukaryotic groups examined for CO_2 fixation – Sixteen experiments were
9 completed in the South Atlantic Ocean in three oceanic regions: the Equatorial convergence
10 region (EQ), Southern subtropical gyre (SG) and Southern temperate region (ST)
11 (Supplementary Fig. 1) to compare representative mean growth rates that should encompass
12 natural variations in cell abundance and nutrient availability. The following cells were flow
13 sorted: *Prochlorococcus* (*Pro*) [13], *Synechococcus* (*Syn*), small plastidic protists (Pl-S, cell
14 diameter ~ 2 µm), large plastidic protists (Pl-L, cell diameter ~ 3 µm) [8, 14, 15]. In addition low
15 nucleic acid containing bacterioplankton (LNA) and aplastidic protists (A-Pl, cell diameter ~
16 3 µm) were flow sorted as controls.

17 To compare cellular growth and biomass of the smallest oceanic plastidic protists and
18 cyanobacteria $^{14}CO_2$ fixation by flow cytometrically enumerated and sorted *Pro*, *Syn*, Pl-S
19 and Pl-L cells was measured at the end of the light period (12 h) and at the end of the
20 following 12 h dark period (24 h). The amount of tracer in flow sorted *Pro*, *Syn*, Pl-S and Pl-
21 L cells was generally higher at 12 h than at 24 h, while the opposite was true for A-Pl cells
22 (Supplementary Figs. 2-3). The amount of tracer in flow sorted LNA cells was statistically
23 indistinguishable from the background (Supplementary Fig. 3), indicating that the SAR11
24 alphaproteobacteria, which comprised the LNA cell population [13], did not fix CO_2. The

increased ^{14}C-radioactivity of the A-Pl cells in the dark has a ready explanation – the A-Pl cells continued feeding on ^{14}C-labelled CO_2 fixers in the dark. The decreased ^{14}C-radioactivity of the *Pro*, *Syn*, Pl-S and Pl-L cells in the dark (Supplementary Fig. 2b-f) can depend on two cellular processes. Firstly, the cells had directly lost carbon fixed during the light period (primarily by respiration but also exudation, egestion or lysis). Secondly, the reduction in cellular radioactivity was a result of cell division, because smaller daughter cells would contain less tracer than the larger parent cells and therefore an increased proportion of daughter cells will decrease average radioactivity per cell in the sampled population.

<u>Dark respiration versus cell division</u> – To assess the magnitude of dark physiological loss of ^{14}C, tracer retention by each population as well as by their sum was compared at 12 and 24 h (Supplementary Fig. 4). Average cellular ^{14}C content was multiplied by corresponding cell concentrations (Supplementary Fig. 5). A statistically significant increase in radioactivity of the A-Pl population between 12 and 24 h (Supplementary Fig. 4b) was a result of A-Pl cells feeding on ^{14}C-labelled phototrophic cells in the dark. No statistically significant difference in the *Pro*, Pl-S and Pl-L populations was found between the two time points indicating that dark respiration of ^{14}C-labelled material in those cells was insignificant. Statistical significance of the decrease in the radioactivity of the *Syn* population (Supplementary Fig. 4e) was more likely due to grazing on *Syn* cells by A-Pl, mixotrophic Pl-S and Pl-L cells [14, 15] than to *Syn* dark respiration, because the $^{14}CO_2$ fixed at 12 and 24 h by the sum of all flow sorted populations (including predators) was similar (Supplementary Fig. 4a).

The above negligibly small dark respiration of ^{14}C-labelled cellular material is in agreement with earlier laboratory experiments on algal cultures [16] with dark respiration being 2-16% of daily fixed CO_2. A 12% value was calculated for nitrate-limited chemostat-growing cultures of *Monochrysis lutheri* [17], when washout from a chemostat was taken into account.

Relative dark respiration for a batch culture of *Isochrysis galbana* grown from nutrient-replete into nutrient-starved conditions was about 4% [18]. For *Skeletonema costatum* grown under nutrient replete conditions at photon flux densities of 50 and 1200 μmol photons m^{-2} s^{-1} dark respiration was 2% and 16% of photosynthesis, respectively [19]. However, there were also reports of considerable dark respiration that accounted for 30-40% of daylight CO_2 fixation in oligotrophic waters [20] and 20-25% of daylight CO_2 fixation in the temperate North Atlantic [21]. The discrepancy between the reported high dark respiration and the presented data (Supplementary Fig. 4) presumably originated from the methodological differences. The published high values were obtained by gently collecting live phytoplankton on filters. In the present study phytoplankton samples were fixed to preserve cell integrity for subsequent flow sorting. Only ^{14}C tracer incorporated into macromolecules remained in fixed cells and ^{14}C tracer incorporated into labile cellular material was released upon fixation, whereas labelled labile material remained in the unfixed cells [22]. Labile material like sugars is preferentially respired by cells [23], whilst turnover of labelled macromolecules in cells is slow [24]. In the present study the dark respiration of macromolecules was examined and found negligibly low (Supplementary Fig. 4) and hence cell division was considered the main process responsible for radiotracer decrease in mean cells in the dark (Supplementary Fig. 2).

Pro and *Syn* as well as the smallest plastidic protists synchronise their cell division after dusk [25-29] (M.V.Z. unpublished observations). Therefore assumption of night cell division is plausible. This means that only the difference between divisions in the first 12 light hours and the subsequent 12 dark hours can be determined. Accordingly, the derived growth rates are conservative estimates.

Group-specific growth rates – The observed increases in concentrations of cells between 12 and 24 h (Supplementary Fig. 5) were used to independently assess group-specific growth

1 rates for comparison with the rates determined using the ^{14}C tracer method. The growth rates
2 of the Pl-S and Pl-L, estimated by the two methods, were statistically similar (Supplementary
3 Fig. 6), proving that the tracer method gave realistic estimates of growth rates of plastidic
4 protists.

5 The tracer-derived growth rates of the *Pro* and *Syn* were 2-4 times higher than their
6 cell-derived growth rates. This discrepancy can be reconciled if cyanobacteria either have
7 high rates of dark respiration, or are under strong mortality pressure. In the first case mean
8 dark respiration should be >50% for *Pro* and *Syn* in the SG+EQ and EQ, respectively, and
9 80% for *Syn* in the ST. These high values are unlikely (see above, Supplementary Fig. 4e,f).
10 The increased radioactivity of the A-Pl in the dark (Supplementary Figs. 2a, 4b), and similar
11 radioactivity of the sum (Supplementary Fig. 4a) support grazing on cyanobacteria by the A-
12 Pl, Pl-L and Pl-S. Those grazing-related ^{14}C retentions would reduce the tracer-based
13 estimates of growth rates of Pl-S and Pl-L. Indeed, their tracer-derived growth rates showed a
14 trend of being lower than their cell-derived growth rates (Supplementary Fig. 6); however,
15 the differences were statistically insignificant, suggesting that phototrophic CO_2 fixation is
16 the main contributor to the growth of Pl-L and Pl-S cells. Accordingly, grazing being the
17 main cause of the difference between the tracer-derived and cell-derived growth rates of the
18 *Pro* and *Syn* (Supplementary Fig. 6), the former estimated the intrinsic growth of
19 cyanobacteria whereas the latter estimated the net growth of cyanobacteria.

20 <u>Comparison of the growth rates of the CO_2 fixers</u> – The region-averaged growth rates of the
21 studied groups ranged between 0.1 and 0.6 d^{-1} (Fig. 1). The *Syn* grew fastest in the EQ
22 regions, 0.7 d^{-1}; however, these data were omitted from the figure as unrepresentative for the
23 combined EQ+SG regions, because *Syn* growth was not determined in the SG region owing
24 to their low cell concentrations (Supplementary Fig. 1b). The growth rates of *Pro* in the EQ

1 (0.3-0.6 d^{-1}) are similar to *Pro* growth rates determined at the base of the photic layer in the
2 Sargasso Sea [30] and in agreement with rates of up to one doubling per day, determined in the
3 equatorial Pacific using cell cycle analysis [25]. The mean growth rates of *Syn* in the ST and
4 *Pro* in the EQ+SG were, respectively, three and two times higher than the mean growth rates
5 of Pl-L or Pl-S (Supplementary Fig. 6). Therefore, the growth rates of both cyanobacteria in
6 all regions studied were significantly higher than the growth rates of the smallest plastidic
7 protists.

8 The finding that plastidic protists have lower growth rates than cyanobacteria (Fig. 1)
9 requires reconciliation with the hypothesis of optimal cell size to achieve maximum
10 photosynthetic growth [4, 5]. In the present study the smallest eukaryotes showed growth rates
11 (Fig. 1, Supplementary Fig. 6) of one half or less compared to the growth rates of eukaryotes
12 of comparable size in nutrient-rich culture [5]. If the taxon-independent approach is applied the
13 above suggests that eukaryotes are underperforming in the oligotrophic open ocean, being
14 poorly adapted to their habitat. An alternative explanation could be that the eukaryotes
15 cultured in the laboratory are physiologically different from the eukaryotes inhabiting the
16 open ocean, for example the latter are mixotrophs underrepresented in culture collections but
17 capable of outcompeting obligate phototrophs in nature[31]. If this is correct, the difference
18 between potential and realised growth rates is as likely to be related to physiological
19 divergence as to evolutionary inadequacy.

20 There is more controversy about the *in situ* growth rates of the *Pro* and *Syn* in the EQ
21 (Figs. 1-2, Supplementary Fig. 6) being about twice as high as their growth rates in the
22 nutrient unlimited culture at similar light intensity [5]. Because the *in situ* rates cannot be
23 higher than the maximum rates, it is probable that either low temperature of 18°C or high

1 nutrient conditions in culture experiments were less optimal for the cyanobacterial growth
2 than the low nutrient conditions in the open ocean.
3 Fixation rates and biomasses of the CO_2 fixers – The cellular CO_2 fixation rates of the studied
4 groups span four orders of magnitude in direct proportion to their cellular biomasses (Fig.
5 3a). The average fixation rates of the Pl-L and Pl-S cells were statistically similar in all
6 regions and the average fixation rates of the *Syn* cells were comparable in the EQ and ST
7 regions. Being more sensitive to nutrient conditions, the cellular CO_2 fixation rates of
8 cyanobacteria were more variable than the rates of eukaryotes (Supplementary Fig. 2).
9 The average biomass of *Pro* and *Syn* cells was 60% lower and the biomass of Pl-S and Pl-L
10 was 20-120% higher according to the tracer method compared to the biovolume method [11, 15]
11 (Fig. 3a). Firstly, it was reassuring that the estimates based on the two independent
12 approaches were comparable. Secondly, because *Pro* and *Syn* cell diameters were estimated
13 by size fractionation using broad-stepped (0.2 µm) pore size filters it was unsurprising that
14 the biovolume-based method gave higher biomass estimates. Thirdly, the microscopic size
15 measurements of fixed and consequently shrunk Pl-S and Pl-L cells using nucleic acid-
16 specific stain would underestimate the living cell sizes. Hence, cellular biomass, estimated
17 using the sensitive ^{14}C-tracer method, is more likely to be closer to the real biomass of living
18 cells. Among the studied groups *Pro* cells were the smallest (Fig. 3a). Taking a 1.7 Mbp
19 genome size of *Pro* MED4 strain for guidance [32], the *Pro* chromosome would constitute 5%
20 of cellular biomass, which is within the theoretical limits [4] for a viable phototrophic cell.
21 Within the limited size range of the studied microbes a relationship between the
22 cellular biomass and biomass growth rate indicates a slope difference between the
23 cyanobacteria and smallest plastidic protists (Fig. 2). The slope drop from prokaryotes to
24 eukaryotes is in agreement with the step shift during a transition from heterotrophic

1 prokaryotes to protozoa [33], suggesting similarity in bioenergetic scaling between phototrophic
2 and heterotrophic microbes. Such similarity could be linked to commonness of versatile
3 metabolism among oceanic CO_2-fixing microbes – mixotrophy of the smallest eukaryotes [15]
4 and photoheterotrophy of cyanobacteria [13].

5 At the population level the biomasses of the *Pro* and *Syn* were, respectively, 40% and
6 20% of the biomass of the Pl-L (Fig. 3b), or merely 25% of the sum of Pl-L, Pl-S and *Pro* in
7 the EQ+SG and 13% of Pl-L, Pl-S and *Syn* in the ST. Daily CO_2 fixation by the *Pro* and *Syn*
8 populations equated to 80% of the fixation by the Pl-L population, or 40% and 35% by the
9 corresponding sums. Although eukaryotes clearly dominated the biomass of the CO_2 fixers in
10 the studied regions, cyanobacterial populations fixed CO_2 more effectively and grew faster. If
11 grazing control by eukaryotes was relaxed, cyanobacterial populations could outgrow
12 populations of plastidic protists within days because of faster cyanobacterial reproduction.

13 **Discussion**

14 It seems that after $>10^9$ years of co-evolution [34] the smallest phototrophic eukaryotes have not
15 succeeded in exceeding the growth of cyanobacteria in the oligotrophic open ocean.
16 However, if, in addition to competing for major inorganic nutrients, eukaryotes feed on
17 bacteria [14, 35, 36], then eukaryote survival as predators would depend on growth of
18 phototrophic prokaryotes. The nutritional adaptations of photrophic eukaryotes and
19 prokaryotes in the nutrient-depleted open ocean have established, perhaps, the simplest
20 ecosystem of faster growing photoheterotrophic prokaryotes largely controlled by
21 mixotrophic eukaryotes.
22

Methods

Sampling – The experimental study was carried out on board the UK Royal Research Ship (RRS) *James Cook* during the Atlantic Meridional Transect (AMT) cruise number JC079 (AMT22) in October-November 2012. Seawater samples were collected before dawn with 20-litre Niskin bottles mounted on the sampling rosette of a conductivity-temperature-depth profiler (Sea-Bird Electronics, Washington, USA) from a depth of 20 m, a representative depth of the surface mixed layer unaffected by the ship's movement and contamination. Samples were gently transferred into a 10L polypropylene carboy, before being dispensed through a spigot into 120 ml Pyrex glass bottles. All plastic- and glass-ware was soaked in 10% HCl and extensively rinsed with sampled seawater. All experiments were set up within 20 minutes after sample collection.

CO_2 fixation experiments – To assess the effect of high $NaH^{14}CO_3$ tracer addition, necessary to determine CO_2 fixation rates by the tiniest phototrophic prokaryote – *Prochlorococcus* cyanobacteria [30], radiotracers of two manufacturers were used. Sodium bicarbonate as a solution (Perkin-Elmer, USA) was added directly to sampled seawater, whilst crystals of sodium bicarbonate (Hartmann Analytic, Germany), were dissolved in autoclaved seawater, collected from 20 m depth (the latter tracer gave on average 12% higher estimates of CO_2 fixation than the former one – data not shown). Working solutions of both radiotracers were filtered through a 0.2 µm pore size filter before being added to sampled seawater (90-240 kBq ml^{-1} final radioactivity). The bottled samples were then incubated at ambient temperatures controlled by a refrigerated water bath (Grant Instruments, UK) in a 6L acrylic glass water tank illuminated by a warm white light-emitting diode array (Photon Systems Instruments, Czech Republic) adjusted to 350 µmol photons m^{-2} s^{-1}, mimicking the average in situ light conditions at 20 m depth in subtropical waters. The constant light output was used

1 to allow direct comparison of cellular CO_2 fixation determined in experiments with seawater
2 samples collected at different latitudes. After 12 h incubation in the light, to mimic the day
3 period, 60 ml of sample were poured into a polypropylene bottle containing 3 ml of 20%
4 paraformaldehyde (PFA, final concentration 1%). PFA solution was prepared by dissolving
5 PFA powder in seawater by stirring on a heating plate followed by filtering of cooled solution
6 through a 0.2 µm pore size filter. The Pyrex bottles containing the remaining 60 ml of sample
7 were transferred into a parallel, temperature-controlled, light-tight 6L tank and incubated for
8 an additional 12 h in the dark at ambient temperature to mimic the night period. At the end of
9 the experiment the remaining 60 ml of sample were fixed with 1% PFA. CO_2 fixation in dark
10 controls were <2% of CO_2 fixation in the 12 h light incubations (e.g. 0.18±0.01 mg C m^{-3} d^{-1}
11 in the dark versus 9.68±0.84 mg C m^{-3} d^{-1} in the light at 4°1.8'N, 26°28.2'W).
12 Subsamples were taken from each polypropylene bottle containing a fixed sample to
13 determine the total CO_2 fixation and the exact amount of added radiotracer. Three 1.6 ml
14 subsamples were transferred into 2 ml microcentrifuge tubes to determine absolute
15 concentrations of microbial populations (see below) and to flow sort *Prochlorococcus* cells,
16 when their natural abundance was sufficiently high to sort at a rate of 150-300 cells min^{-1}. A
17 single 20 ml subsample was concentrated using a 0.4 µm polycarbonate filter (Nuclepore,
18 Whatman, UK) mounted in a filtration unit (Swinnex, Millipore, USA) using a syringe pump
19 (KD Scientific, USA) at a flow rate of 2.0 ml min^{-1} and used for sorting stained
20 *Prochlorococcus* and *Synechococcus* cells as well as small plastidic protists. The remaining
21 sample was concentrated using a 0.6 µm Nuclepore polycarbonate filter in the same way for
22 flow sorting large plastidic protists and aplastidic protists. The seawater retained inside the
23 filtration units as well as the filters were transferred into 2 ml microcentrifuge tubes. The
24 unconcentrated subsamples and two concentrated subsamples of the same 1.6 ml final

volume, were stained inside the microcentrifuge tubes with SYBR Green I (Sigma-Aldrich, UK) in three potassium citrate buffer [37, 38] and flow sorted within 24 h. Stained samples scheduled for sorting were stored in the dark at 4°C.

Flow cytometric sorting – Stained microbial cells from different populations were discriminated, enumerated and flow sorted using a FACSCalibur flow cytometer (Becton Dickinson, Oxford, UK). An internal standard of 0.5 µm and 1.0 µm diameter, multi-fluorescent beads (Polysciences, Germany) was added to each stained sample prior to analyses to monitor instrument performance and to determine absolute concentrations of microbial populations [38, 39].

For each flow-sorted population 4-6 replicates of different cell numbers were sorted (e.g. Supplementary Fig. 3). Bacterial and eukaryotic cells were collected on 0.2 µm and 0.8 µm polycarbonate filters, respectively, using a three socket filtration unit and prepared for radio-assaying following the same procedure as for total carbon fixation measurements. Using a liquid scintillation counter (Tri-Carb 3100, Perkin Elmer, UK) samples (a sample was counted for 5 min) from each experiment were batch counted 3-4 times on different days. To account for counting variations a mean of these 3-4 counts was calculated before a relative average cellular rate of CO_2 fixation was computed as a fraction of the amount of radiotracer added to the experimental bottle. To enable comparison of measured cellular CO_2 fixation rates between experiments absolute fixation rates were calculated.

CO_2 concentrations in sampled seawater, derived from the CTD measurements of seawater salinity [40] were used to convert relative cellular rates of CO_2 fixation into absolute CO_2 fixation rates in units of gram carbon fixed by an average cell of the flow sorted population. The CO_2 fixation of flow sorted *Pro*, *Syn*, Pl-S or Pl-L cells was determined experimentally as a mean cellular daily growth rate C^{fix}_{12} [g C cell^{-1} d^{-1}]. The CO_2 fixation

1 C^{fix}_{24}, determined at 24 h, is a mean for the fraction of cells that divided during the dark
2 period (D^{div}) and the ones that remained undivided. The divided cells double in number but
3 each cell contains a half of the fixed CO_2. This simple model can be described by the
4 following formula:

5 $$C^{fix}_{24} = (2 \times D^{div} \times C^{fix}_{12} / 2 + (1 - D^{div}) \times C^{fix}_{12}) / (1 + D^{div}) \quad (1)$$

6 The above formula can be simplified and re-arranged to calculate the daily relative growth
7 rate D^{div} [d^{-1}] assuming that cells divided during the dark period:

8 $$D^{div} = (C^{fix}_{12} - C^{fix}_{24}) / C^{fix}_{24} \quad (2)$$

9 Then the cellular biomass C^{biom} [g C $cell^{-1}$] could be computed:

10 $$C^{biom} = C^{fix}_{12} / D^{div} \quad (3)$$

11 or

12 $$C^{biom} = C^{fix}_{12} \times C^{fix}_{24} / (C^{fix}_{12} - C^{fix}_{24}) \quad (4)$$

13 The F-test was used for analyses of variance and the paired t-test was used for comparing
14 means or alternatively Wilcoxon signed rank test was used in cases when normality test failed
15 ($P<0.05$). Standard errors of mean were propagated when growth rates, biomasses,
16 population-specific CO_2 fixation rates were calculated.
17

1 **Acknowledgements**

2 I thank Glen Tarran (the chief scientist), fellow scientists, technicians, captain, officers and
3 crew aboard the RRS *James Cook* for their support during the cruise. I gratefully
4 acknowledge Michael Sleigh, Richard Geider, Adrian Martin and three anonymous reviewers
5 for their critical comments on earlier drafts of the paper. This study was supported by the UK
6 Natural Environment Research Council (NERC) through the core funding of the National
7 Oceanography Centre as well as through the Research Grant NE/H005196/1, and the
8 European Commission Seventh Framework Programme through the GreenSeas Collaborative
9 Project (FP7-ENV-2010 Contract 265294). This is Atlantic Meridional Transect publication
10 number 248.

11

1 **References**

2 1 Kirchman, D. L. Carbon cycle – microbial breathing lessons. *Nature* **385**, 121-122 (1997).

3 2 Falkowski, P. G., Fenchel, T. & Delong, E. F. The microbial engines that drive Earth's
4 biogeochemical cycles. *Science* **320**, 1034-1039 (2008).

5 3 Lane, N. & Martin, W. The energetics of genome complexity. *Nature* **467**, 929-934
6 (2010).

7 4 Raven, J. A. Why are there no picoplanktonic O_2 evolvers with volumes less than 10^{-19}
8 M^3? *J. Plankton Res.* **16**, 565-580 (1994).

9 5 Maranon, E. *et al.* Unimodal size scaling of phytoplankton growth and the size
10 dependence of nutrient uptake and use. *Ecol. Lett.* **16**, 371-379 (2013).

11 6 Worden, A. Z., Nolan, J. K. & Palenik, B. Assessing the dynamics and ecology of marine
12 picophytoplankton: The importance of the eukaryotic component. *Limnol. Oceanogr.* **49**,
13 168-179 (2004).

14 7 Li, W. K. W. Primary production of prochlorophytes, cyanobacteria, and eukaryotic
15 ultraphytoplankton - measurements from flow cytometric sorting. *Limnol. Oceanogr.* **39**,
16 169-175 (1994).

17 8 Jardillier, L., Zubkov, M. V., Pearman, J. & Scanlan, D. J. Significant CO_2 fixation by
18 small prymnesiophytes in the subtropical and tropical northeast Atlantic Ocean. *ISME*
19 *Journal* **4**, 1180-1192 (2010).

20 9 Chisholm, S. W. in *Primary productivity and biogeochemical cycles in the sea* (eds P. G.
21 Falkowski & A. D. Woodhead) 213-237 (Plenum Press, 1992).

22 10 Banavar, J. R., Damuth, J., Maritan, A. & Rinaldo, A. Supply-demand balance and
23 metabolic scaling. *Proc. Natl. Acad. Sci.* **99**, 10506-10509 (2002).

1 11 Zubkov, M. V., Sleigh, M. A., Burkill, P. H. & Leakey, R. J. G. Picoplankton community
2 structure on the Atlantic Meridional Transect: a comparison between seasons. *Prog.*
3 *Oceanogr.* **45**, 369-386 (2000).
4 12 Christian, J. R. & Karl, D. M. Microbial community structure at the United-States Joint
5 Global Ocean Flux Study Station ALOHA - Inverse methods for estimating biochemical
6 indicator ratios. *J. Geophys. Res.-Oceans* **99**, 14269-14276 (1994).
7 13 Gomez-Pereira, P. R. *et al.* Comparable light stimulation of organic nutrient uptake by
8 SAR11 and *Prochlorococcus* in the North Atlantic subtropical gyre. *ISME Journal* **7**,
9 603-614 (2013).
10 14 Zubkov, M. V. & Tarran, G. A. High bacterivory by the smallest phytoplankton in the
11 North Atlantic Ocean. *Nature* **455**, 224-226 (2008).
12 15 Hartmann, M. *et al.* Mixotrophic basis of Atlantic oligotrophic ecosystems. *Proc. Natl.*
13 *Acad. Sci.* **109**, 5756-5760 (2012).
14 16 Geider, R. J. & Osborne, B. A. Respiration and microalgal growth – a review of the
15 quantitative relationship between dark respiration and growth. *New Phytol.* **112**, 327-341
16 (1989).
17 17 Laws, E. & Caperon, J. Carbon and nitrogen metabolism by *Monochrysis lutheri* –
18 measurement of growth rate dependent respiration rates. *Mar. Biol.* **36**, 85-97 (1976).
19 18 Flynn, K. J., Davidson, K. & Leftley, J. W. Carbon-nitrogen relations at whole-cell and
20 free-amino-acid levels during batch growth of *Isochrysis galbana* (Prymnesiophyceae)
21 under conditions of alternating light and dark. *Mar. Biol.* **118**, 229-237 (1994).
22 19 Anning, T. *et al.* Photoacclimation in the marine diatom *Skeletonema costatum*. *Limnol.*
23 *Oceanogr.* **45**, 1807-1817 (2000).

1 20 Geider, R. J. in *Primary Productivity and Biogeochemical Cycles in the Sea* (ed P.
2 Falkowski) 333-360 (Plenum Press, 1992).
3 21 Marra, J. & Barber, R. T. Phytoplankton and heterotrophic respiration in the surface layer
4 of the ocean. *Geophys. Res. Lett.* **31**, doi:10.1029/2004gl019664 (2004).
5 22 Zubkov, M. V. & Leakey, R. J. G. Evaluation of the efficiency of metabolism of
6 dinoflagellate phosphorus and carbon by a planktonic ciliate. *Eur. J. Protistol.* **45**, 166-
7 173 (2009).
8 23 Glover, H. E. & Morris, I. Photosynthetic characteristics of coccoid marine cyanobacteria.
9 *Archives of Microbiology* **129**, 42-46 (1981).
10 24 Zubkov, M. V., Sleigh, M. A. & Burkill, P. H. Measurement of bacterivory by protists in
11 open ocean waters. *FEMS Microbiol. Ecol.* **27**, 85-102 (1998).
12 25 Vaulot, D., Marie, D., Olson, R. J. & Chisholm, S. W. Growth of *Prochlorococcus*, a
13 photosynthetic prokaryote, in the equatorial Pacific Ocean. *Science* **268**, 1480-1482
14 (1995).
15 26 Vaulot, D. & Marie, D. Diel variability of photosynthetic picoplankton in the equatorial
16 Pacific. *J. Geophys. Res.-Oceans* **104**, 3297-3310 (1999).
17 27 Wyman, M. Diel rhythms in ribulose-1,5-bisphosphate carboxylase/oxygenase and
18 glutamine synthetase gene expression in a natural population of marine picoplanktonic
19 cyanobacteria (*Synechococcus* spp.). *Appl. Environ. Microbiol.* **65**, 3651-3659 (1999).
20 28 Zubkov, M. V., Sleigh, M. A. & Burkill, P. H. Assaying picoplankton distribution by flow
21 cytometry of underway samples collected along a meridional transect across the Atlantic
22 Ocean. *Aquat. Microb. Ecol.* **21**, 13-20 (2000).

1 29 Zubkov, M. V. & Quartly, G. D. Ultraplankton distribution in surface waters of the
2 Mozambique Channel - flow cytometry and satellite imagery. *Aquat. Microb. Ecol.* **33**,
3 155-161 (2003).
4 30 Chisholm, S. W. *et al.* A novel free-living prochlorophyte abundant in the oceanic
5 euphotic zone. *Nature* **334**, 340-343 (1988).
6 31 Tittel, J. *et al.* Mixotrophs combine resource use to outcompete specialists: Implications
7 for aquatic food webs. *Proc. Natl. Acad. Sci.* **100**, 12776-12781 (2003).
8 32 Lamerdin, J. & al. *Prochlorococcus marinus* MED4 Genome Project Completed Genome.
9 *http://www.jgi.doe.gov* (2001).
10 33 DeLong, J. P., Okie, J. G., Moses, M. E., Sibly, R. M. & Brown, J. H. Shifts in metabolic
11 scaling, production, and efficiency across major evolutionary transitions of life. *Proc.*
12 *Natl. Acad. Sci.* **107**, 12941-12945 (2010).
13 34 Knoll, A. H., Javaux, E. J., Hewitt, D. & Cohen, P. Eukaryotic organisms in Proterozoic
14 oceans. *Philos. Trans. R. Soc. London B* **361**, 1023-1038 (2006).
15 35 Frias-Lopez, J., Thompson, A., Waldbauer, J. & Chisholm, S. W. Use of stable isotope-
16 labelled cells to identify active grazers of picocyanobacteria in ocean surface waters. *Env.*
17 *Microbiol.* **11**, 512-525 (2009).
18 36 Hartmann, M., Zubkov, M. V., Scanlan, D. J. & Lepere, C. In situ interactions between
19 photosynthetic picoeukaryotes and bacterioplankton in the Atlantic Ocean: evidence for
20 mixotrophy. *Environmental Microbiology Reports* **5**, 835-840 (2013).
21 37 Marie, D., Partensky, F., Jacquet, S. & Vaulot, D. Enumeration and cell cycle analysis of
22 natural populations of marine picoplankton by flow cytometry using the nucleic acid stain
23 SYBR Green I. *Appl. Environ. Microbiol.* **63**, 186-193 (1997).

1 38 Zubkov, M. V., Burkill, P. H. & Topping, J. N. Flow cytometric enumeration of DNA-
2 stained oceanic planktonic protists. *J. Plankton Res.* **29**, 79-86 (2007).
3 39 Zubkov, M. V. & Burkill, P. H. Syringe pumped high speed flow cytometry of oceanic
4 phytoplankton. *Cytom. Part A* **69A**, 1010-1019 (2006).
5 40 Parsons, T. R., Maita, Y. & Lalli, C. M. *Manual of chemical and biological methods for*
6 *seawater analysis*. (Pergamon Press, 1984).
7

1 **Figure legends**

2 **Figure 1. Relative growth rates of phytoplankton groups.** Comparison of the growth rates
3 of large plastidic protists (Pl-L), small plastidic protists (Pl-S), *Prochlorococcus* (*Pro*) and
4 *Synechococcus* (*Syn*) in the two regions: combined Equatorial waters (EQ) and Southern gyre
5 (SG) and Southern temperate waters (ST). Error bars indicate propagated single standard
6 errors.

7 **Figure 2. Metabolic scaling in prokaryotes and eukaryotes.** Scatter plot of biomass versus
8 daily growth of *Prochlorococcus* (*Pro*), *Synechococcus* (*Syn*), small plastidic protists (Pl-S)
9 and large plastidic protists (Pl-L) to compare their growth. Solid lines indicate linear
10 regressions of cyanobacteria (slope=1.4, r^2=0.89, P<0.001) and picoeukaryotes (slope =0.6,
11 r^2=0.67, P<0.001). Dashed line indicates equality of biomass and daily growth.

12 **Figure 3. Absolute biomasses and growth rates of phytoplankton groups.** Comparison of
13 the ^{14}C tracer based estimates of cellular (a) and population (b) biomasses and growth rates
14 (internal intermediate grey bars) of large plastidic protists (Pl-L), small plastidic protists (Pl-
15 S), *Prochlorococcus* (*Pro*) and *Synechococcus* (*Syn*) in the two regions: combined Equatorial
16 waters (EQ) and Southern gyre (SG) and Southern temperate waters (ST). Thin white bars (a)
17 indicate biovolume-based estimates of cellular biomass. Note the log scale of the X-axis.
18 Error bars indicate propagated single standard errors.

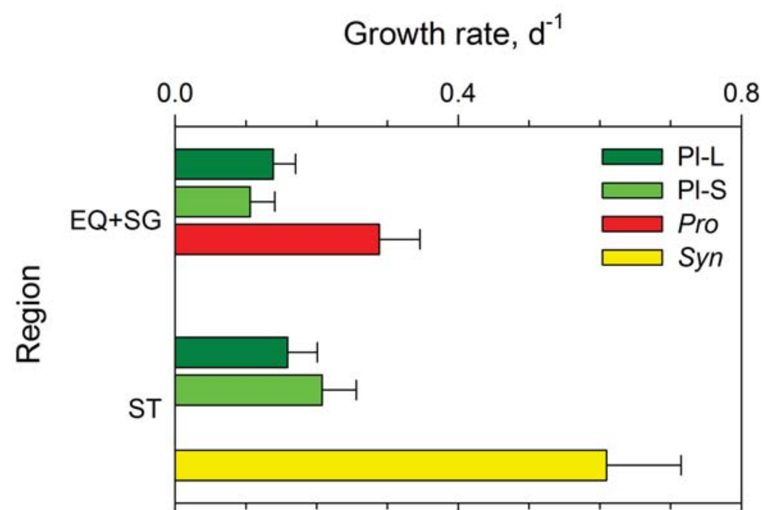
Growth rate, d-1
0.0
0.4
0.8
Region
EQ+SG
ST
Pl-L
Pl-S
Pro
Syn

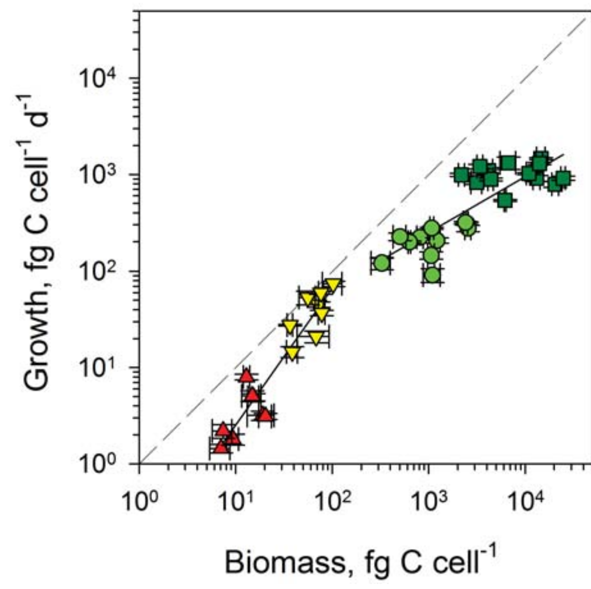

Growth, fg C cell^{-1} d^{-1}
Biomass, fg C cell^{-1}
10^0
10^1
10^2
10^3
10^4

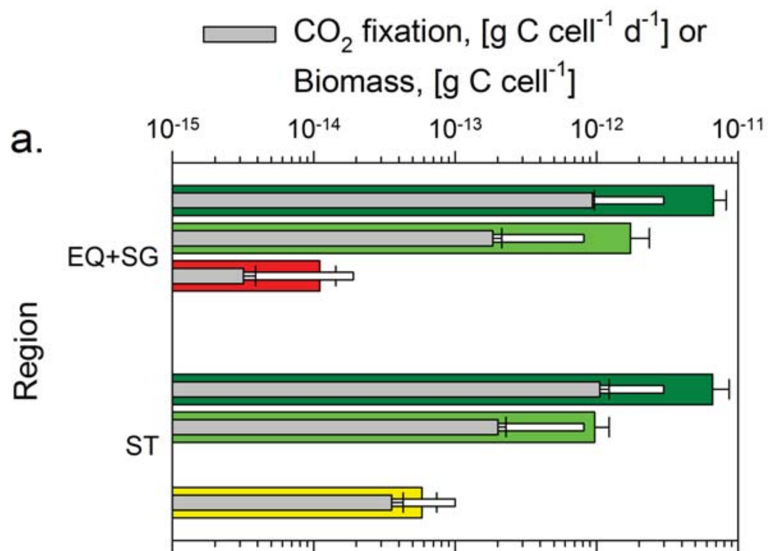

CO_2 fixation, [g C cell^{-1} d^{-1}] or
Biomass, [g C cell^{-1}]
a.
10^{-15}
10^{-14}
10^{-13}
10^{-12}
10^{-11}
EQ+SG
Region
ST

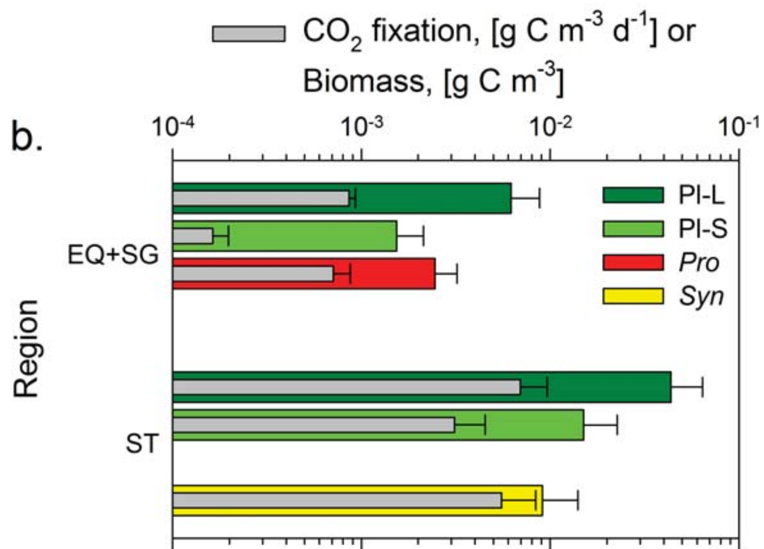

CO_2 fixation, [g C m^{-3} d^{-1}] or
Biomass, [g C m^{-3}]
b.
10^{-4}
10^{-3}
10^{-2}
10^{-1}
EQ+SG
Region
ST
Pl-L
Pl-S
Pro
Syn